1521-0103/362/1/119–130$25.00
THE JOURNAL OF PHARMACOLOGY AND EXPERIMENTAL THERAPEUTICS

https://doi.org/10.1124/jpet.117.240614
J Pharmacol Exp Ther 362:119–130, July 2017

Glutaminyl Cyclase Inhibitor PQ912 Improves Cognition in Mouse Models of Alzheimer's Disease—Studies on Relation to Effective Target Occupancy

Torsten Hoffmann, Antje Meyer, Ulrich Heiser, Stephan Kurat, Livia Böhme, Martin Kleinschmidt, Karl-Ulrich Bühring, Birgit Hutter-Paier, Martina Farcher, Hans-Ulrich Demuth, Inge Lues, and Stephan Schilling

Probiodrug AG, Halle, Germany (T.H., A.M., U.H., L.B., K.-U.B., I.L.); QPS Austria, Grambach, Austria (S.K., B.H.-P., M.F.); and Fraunhofer Institute for Cell Therapy and Immunology, Department for Drug Design and Target Validation, Halle, Germany (M.K., H.-U.D., S.S.)

Received February 7, 2017; accepted April 24, 2017

ABSTRACT

Numerous studies suggest that the majority of amyloid-β (Aβ) peptides deposited in Alzheimer's disease (AD) are truncated and post-translationally modified at the N terminus. Among these modified species, pyroglutamyl-Aβ (pE-Aβ, including N3pE-Aβ40/42 and N11pE-Aβ40/42) has been identified as particularly neurotoxic. The N-terminal modification renders the peptide hydrophobic, accelerates formation of oligomers, and reduces degradation by peptidases, leading ultimately to the accumulation of the peptide and progression of AD. It has been shown that the formation of pyroglutamyl residues is catalyzed by glutaminyl cyclase (QC). Here, we present data about the pharmacological in vitro and in vivo efficacy of the QC inhibitor (S)-1-(1H-benzo[d]imidazol-5-yl)-5-(4-propoxyphenyl)imidazolidin-2-one (PQ912), the first-in-class compound that is in clinical development. PQ912 inhibits human, rat, and mouse QC activity, with K_i values ranging between 20 and 65 nM. Chronic oral treatment of $hAPP_{SL}$xhQC double-transgenic mice with approximately 200 mg/kg/day via chow shows a significant reduction of pE-Aβ levels and concomitant improvement of spatial learning in a Morris water maze test paradigm. This dose results in a brain and cerebrospinal fluid concentration of PQ912 which relates to a QC target occupancy of about 60%. Thus, we conclude that >50% inhibition of QC activity in the brain leads to robust treatment effects. Secondary pharmacology experiments in mice indicate a fairly large potency difference for Aβ cyclization compared with cyclization of physiologic substrates, suggesting a robust therapeutic window in humans. This information constitutes an important translational guidance for predicting the therapeutic dose range in clinical studies with PQ912.

Introduction

Alzheimer's disease (AD) is the most prevalent neurodegenerative disorder. Pathogenic hallmarks of AD are mainly extracellular aggregates of amyloid-β (Aβ) and intracellular neurofibrillary tangles, which are composed of the hyperphosphorylated protein tau (Hardy and Higgins, 1992; Mudher and Lovestone, 2002). Aβ plaques have been shown to poorly predict the cognitive status of patients. Rather, nonfibrillary soluble Aβ oligomers appear to correlate with the development of the disease and to induce tau pathology (Lambert et al., 1998; Selkoe, 2008; Shankar et al., 2008; Ittner and Götz, 2011). These oligomers contain truncated and modified forms of Aβ at a significant extent, as recently shown by Esparza et al. (2016) and discussed at Alzforum (http://www.alzforum.org/print-series/620566).

A substantial degree of Aβ heterogeneity is attributed to the N terminus (Bayer and Wirths, 2014). Among these species, truncated Aβ variants starting at positions 3 or 11 with an N-terminal glutamyl residue are post-translationally modified by pyroglutamyl (pE) formation. Pyroglutamyl-Aβ peptides have been shown to be major constituents of Aβ deposits in sporadic and familial AD (Saido et al., 1995; Miravalle et al., 2005; Piccini et al., 2005). In postmortem tissue, the pE-Aβ content of deposits varies between 10 and 25% or even higher, depending on the methods of Aβ extraction (Näslund et al., 1994; Lemere et al., 1996; Saido et al., 1996; Kuo et al., 1997; Portelius et al., 2010; Wu et al., 2014).

The N-terminal formation of pE renders the Aβ peptide more hydrophobic (Schlenzig et al., 2009, 2012). Furthermore, the pE formation triggers rapid oligomerization, which negatively interferes with synaptic and neuronal physiology as

https://doi.org/10.1124/jpet.117.240614.

ABBREVIATIONS: Aβ, amyloid-β; AD, Alzheimer's disease; ANOVA, analysis of variance; APP, amyloid precursor protein; APP-NLE, APP695 KM595/596NLΔDA597/598; APP-NLQ, APP695 KM595/596NL, ΔDA597/598, E599Q; CSF, cerebrospinal fluid; ELISA, enzyme-linked immunosorbent assay; FA, formic acid; GnRH, gonadoliberin; HBS-P, HEPES buffered saline containing P20 surfactant; HEK293, human embryonic kidney cells; HPG, hypothalamic-pituitary-gonadal; HPT, hypothalamic-pituitary-thyroid; LC-MS/MS, liquid chromatography–tandem mass spectrometry; MWM, Morris water maze; PBD150, 1-(3-(1H-imidazol-1-yl)propyl)-3-(3,4-dimethoxyphenyl)thiourea; pE, pyroglutamyl; PQ912, (*S*)-1-(1H-benzo[d]imidazol-5-yl)-5-(4-propoxyphenyl)imidazolidin-2-one; PT, probe trial; QC, glutaminyl cyclase; T4, thyroxine; TBS, Tris-buffered saline; Tg, transgenic; TRH, thyrotropin-releasing hormone or thyroliberin; TSH, thyrotropin.

captured by, e.g., impairments in long-term potentiation (Nussbaum et al., 2012; Schlenzig et al., 2012). The data suggest that Aβ oligomers formed from N3pE-Aβ structurally differ from those of Aβ(1-42), and it is assumed that these structural modifications constitute the basis for the increased toxicity (Nussbaum et al., 2012; Gillman et al., 2014; Matos et al., 2014). Moreover, the toxic oligomeric structure induced by pE-Aβ might be transmitted to full-length Aβ in a mechanism of molecular priming (Nussbaum et al., 2012). Recent studies also suggest that the abundance of pE-Aβ correlates with the appearance of tau-paired helical filaments (Mandler et al., 2014), and that the concentration of N3pE-Aβ in cortical tissue of postmortem human AD brain samples inversely correlates with the cognitive status of the patients (Morawski et al., 2014). In contrast to the content of unmodified Aβ in plaques, the level of pE-Aβ increases and correlates with disease stages. The modified pE-Aβ is first measurable on the brink from the preclinical to clinical stage (Rijal Upadhaya et al., 2014; Thal et al., 2015). These results link the formation and accumulation of N3pE-Aβ to the cognitive status and disease progression of AD. The size and structure of native Aβ oligomers is currently being intensively investigated.

The formation of pE-Aβ is catalyzed by the metal-dependent enzyme glutaminyl cyclase (QC) (Schilling et al., 2004). QC is highly expressed in the human brain and has been shown to be upregulated in AD (Schilling et al., 2008), thereby causing an increase in pE-Aβ formation. Likewise, the concomitant accumulation of Aβ also favors formation of pE-Aβ due to increased QC substrate levels. Previous studies showed that expression of human QC in amyloid precursor protein (APP) transgenic mice increases pE-Aβ formation and induces a behavioral deficit (Jawhar et al., 2011; Nussbaum et al., 2012), whereas a depletion of murine QC prevents the development of the AD-like phenotype in 5xFAD transgenic mice (Jawhar et al., 2011). A pharmacological proof of principle has been shown previously in two different AD mouse models using the QC inhibitor PBD150 [1-(3-(1H-imidazol-1-yl)propyl)-3-(3,4-dimethoxyphenyl)thiourea] as a tool compound. The compound prevents the generation of pE-Aβ(3-42) and improves spatial learning and memory (Schilling et al., 2008).

Within a comprehensive drug discovery program (Buchholz et al., 2006, 2009; Ramsbeck et al., 2013), PQ912 [(*S*)-1-(1H-benzo[d]imidazol-5-yl)-5-(4-propoxyphenyl)imidazolidin-2-one] (Fig. 1) has been selected as a development candidate based on its excellent overall drug-like profile. PQ912 is a first-in-class inhibitor of glutaminyl cyclases currently in clinical development (Lues et al., 2015).

In this paper, we summarize key primary and secondary pharmacological data relevant to evaluating the compound's in vivo efficacy and target occupancy as well as the in vivo substrate selectivity of PQ912 as a basis for the translational assessment of the therapeutic window. The data support a favorable profile of the compound for QC engagement coupled to a reduction of pE-Aβ and behavioral improvements, setting the cornerstones for translation of the approach to clinical trials.

Materials and Methods

Materials

Human and murine QCs were heterologously expressed in *Pichia pastoris* and purified as described previously (Schilling et al., 2002a, 2005). PQ912*HCl was synthesized and purchased from Carbogen Amcis AG (Aarau, Switzerland). For in vitro studies, the drug was dissolved in dimethylsulfoxide (10 mM) and further diluted in the appropriate buffer. For in vivo studies, PQ912 was applied in pelleted standard rodent chow (R/M 10 mm, Ssniff Spezialdiäten, Soest, Germany).

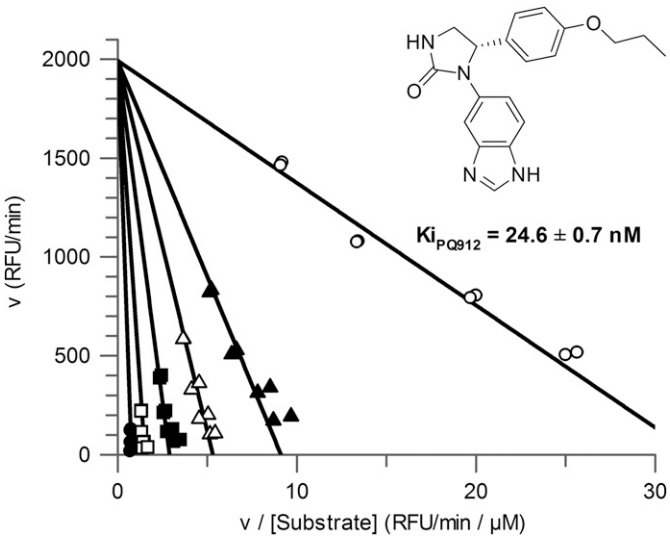

Fig. 1. Eadie-Hofstee plot of PQ912-dependent inhibition of human glutaminyl cyclase. Open circles are values without inhibitor at four concentrations of glutaminyl-7-amido-4-methylcoumarin (20, 40, 80, 160 μM). PQ912 (molecular weight: 336.4 g/mol) was serially diluted from 1000 nM (black circles) to 62.5 nM (black triangles). Nontransformed data were fitted by nonlinear regression (GraFit V5.0.13, Erithacus Software) using the equation for competitive inhibition. The calculated K_i ± S.E. of this experiment is given. RFU, relative fluorescence units.

Animals

hAPP$_{SL}$xhQC (mice double transgenic for the human APP gene containing Swedish and London mutation and human QC, Nussbaum et al., 2012) and 5xFADxhQC transgenic mice (mice transgenic for the human APP gene containing Swedish, Florida and London mutation, the human PS1 gene variant (M146L, L286V) and human QC, Jawhar et al., 2011) were used to assess the efficacy of PQ912. Animals were housed in individually ventilated cages on standardized rodent bedding supplied by Rettenmaier Austria GmbH & Co.KG (Vienna, Austria). Mice were kept in the Association for Assessment and Accreditation of Laboratory Animal Care–accredited animal facility of QPS Austria GmbH (previously JSW Lifesciences, GmbH, Grambach, Austria). Animal studies conformed to the Austrian guidelines for the care and use of laboratory animals and were approved by the Styrian government, Austria (Approval numbers: FA10A-78-Jo45-2009; FA10A-78-Jo58-2010; FA10A-78-Jo88-2011; FA10A-78-Jo89-2011). The room temperature during the study was maintained at approximately 24°C, and the relative humidity was maintained between 40 and 70%. Animals were housed under a constant light cycle (12 hours light/dark). Dried pelleted standard rodent chow (Sniff R/M 10 mm) with or without PQ912 and normal tap water were available to the animals ad libitum. Each animal was checked regularly for any clinical symptoms, and body weight and food consumption of the animals were measured once a week.

Mice of both genders were used in all studies using hAPP$_{SL}$xhQC. Wild-type controls were used only in experiments with behavioral assessment to ensure that the transgenic animals show a behavioral phenotype. For the longitudinal characterization of the double-transgenic APP$_{SL}$/hQC mouse model, only the respective single-transgenic models were used as adequate controls. With regard to 5xFADxhQC, our earlier studies were done in female mice only

(Jawhar et al., 2011). To reconcile with these observations, only female 5xFADxhQC mice were used here again.

In Vitro Binding Studies

The inhibition of recombinant glutaminyl cyclase by PQ912 was assessed at two different pH values (pH 6.0 and pH 8.0) using a coupled assay (Schilling et al., 2002b). The fluorogenic substrate glutaminyl-7-amido-4-methylcoumarin (Bachem, Bubendorf, Switzerland) was applied. Each K_i determination was carried out with four substrate concentrations (range: 0.25–4 K_m) and six inhibitor concentrations. The reactions were performed in 50 mM Tris-HCl, pH 8.0 (or 50 mM 4-morpholineethanesulfonic acid, pH 6.0), and contained 0.4 U/ml recombinant pyroglutamyl aminopeptidase from *Bacillus amyloliquefaciens* (Qiagen, Hilden, Germany) as an auxiliary enzyme. An excitation/emission wavelength of 380/460 nm was used to determine the released 7-amido-4-methylcoumarin. Reactions were started by addition of QC. The activity was determined from a standard curve of the fluorophore under assay conditions. All determinations were carried out at 30°C by using a fluorescence microplate reader (Genios Pro; Tecan, Crailsheim, Germany). Evaluation of kinetic data was performed with GraFit (version 5.0.4 for Windows; Erithacus Software Ltd., Horley, UK). Experimental data were fitted using a competitive binding model.

Binding characteristics of PQ912 to human QC were further investigated using surface plasmon resonance. Human recombinant QC was covalently bound to a CM5 chip (Biacore, Freiburg, Germany). PQ912 was freshly dissolved in 100% dimethylsulfoxide and diluted to 500, 200, 100, 50, 20, 10, 5, and 2 nM in HBS-P (HEPES buffered saline containing P20 surfactant, 0.01 M HEPES pH 7.4, 0.15 M NaCl, 0.005% v/v Surfactant P20). The binding analysis was performed with a flow of 30 μl/min using HBS-P buffer. For each concentration, a sensogram was recorded for 30 minutes. The association was determined by injection of 150 μl of the inhibitor solution (contact time: 5 minutes) with the appropriate concentration using the "KINJECT" command. The dissociation was observed by running HBS-P over the chip surface (including 300-second holding time directly after finishing the injection). Afterward, the chip surface was regenerated by injection of 15 μl of 10 mM sodium acetate, pH 4.0. After injection of 300 μl of activation buffer (25 mM Bis-Tris, 100 mM NaCl, pH 6.8, containing traces of zinc ions for reactivation of the human QC), the chip was equilibrated with HBS-P for 5 minutes before starting a new binding cycle. Determination of the association and dissociation rate and the dissociation constant was performed with BIAevaluation software (V4.1, Biacore/GE Healthcare, Freiburg Germany) by a simultaneously fit of association and dissociation phase over all recorded QC inhibitor concentrations using the "1:1 Langmuir binding" model.

Cellular Assay

The in vitro efficacy of PQ912 was assessed using a cellular model testing the compound's potency to inhibit production of pE-Aβ (Cynis et al., 2008). Mycoplasma-free human embryonic kidney cells (HEK293; DMSZ, Braunschweig, Germany) were cultured in Dulbecco's modified Eagle's medium (10% fetal bovine serum) in a humidified atmosphere of 5% CO_2 at 37°C. Cells were transfected with pcDNA plasmid vectors mediating the expression of human APP variants APP-NLE (APP695 KM595/596NLΔDA597/598) and APP-NLQ (APP695 KM595/596NL, ΔDA597/598, E599Q), essentially as described by Cynis et al. (2008). These constructs were first described by Shirotani and coworkers (2002), and the corresponding Aβ sequences are shown in Table 2. In brief, the constructs mediate the formation of Aβ(3-40/42), or Aβ(3[E→Q]-40/42) by β- and γ-secretase. The N-truncated peptides result from deletions of codons for Asp597 and Ala598, leading to a β-secretase cleavage at position 3 of Aβ. All APP695 variants carried the "Swedish" mutation KM595/596NL to facilitate BACE1 cleavage at the β-site, disfavoring generation of Aβ (11-40/42). HEK293 cells were transfected using Lipofectamin2000 (Invitrogen, Darmstadt, Germany) according to the manufacturer's manual. Transiently transfected cells were grown overnight and afterward were incubated for 24 hours with phenol red–free Dulbecco's modified Eagle's medium (Gibco, Darmstadt, Germany) under serum-free conditions either in the absence or presence of PQ912 at different concentrations. The next day, media were collected, rapidly mixed with protease inhibitor cocktail (Roche, Basel, Switzerland) containing an additional 1 mM PefaBloc (Carl Roth, Karlsruhe, Germany), and stored at −80°C. The cell count of each well was determined using the CASY cell counter system (Scharfe System, Reutlingen, Germany). Aβ(x-40) and N3pE-Aβ40 concentrations were determined using specific sandwich enzyme-linked immunosorbent assays (ELISAs; IBL-Hamburg, Hamburg, Germany) according to the manufacturer's advice.

In Vivo Pharmacology

The in vivo efficacy of PQ912 was assessed by analyzing its effects on lowering the burden of pE-modified Aβ and on spatial learning and memory using the Morris water maze test (MWM). PQ912 dosages were 0.24-, 0.8-, and 2.4-g/kg food pellets. Taking a mean animal weight of 20 g and a daily food consumption of about 5 g as a base, these concentrations correspond to maximal doses of 60, 200, and 600 mg/kg/day, respectively.

Preventive Long-Term Treatment Regimen. Three groups of male and female $hAPP_{SL}$xhQC double-transgenic mice received PQ912 (0.24, 0.8, and 2.4-g/kg food pellets) for 6 months starting at 3 months of age. The wild-type group and transgenic (Tg) control group received drug-free food pellets. The effect of the test compound on learning and memory (MWM) was evaluated at approximately 8.5 months of age. Mice were sacrificed at the age of 9 months and the brain amyloid burden was quantified, applying ELISA for N3pE-Aβ as described later.

Therapeutic Short-Term Treatment Regimen. Male and female $hAPP_{SL}$xhQC double transgenic mice received PQ912 food pellets (0.8 g/kg) for 5 weeks, starting at 7.5 months of age. Animals of the Tg control group received regular food pellets. The effect of the test compound on learning and memory (MWM) was evaluated at approximately 8.5 months of age. Mice were sacrificed at the age of 9 months, and the brain amyloid burden was quantified.

Therapeutic Long-Term Treatment Regimens. Male and female $hAPP_{SL}$xhQC double-transgenic mice received PQ912 food pellets (0.8 g/kg) for 4 months, starting at 8 months of age. Tg controls received normal food pellets. Tg animals of the control group and non-Tg littermates received drug-free food pellets. Mice were sacrificed at the age of 12 months. The brain amyloid burden was quantified, applying ELISA for N3pE-Aβ.

Female 5xFADxhQC mice (Jawhar et al., 2011) received PQ912 orally at doses of 0.8- and 2.4-g/kg food pellets. Treatment was started at 3 months of age. Animals were sacrificed at 6 months of age.

MWM. The Morris water maze consisted of a white circular pool (diameter: 100 cm) filled with tap water at a temperature of 21 ± 2°C. The pool was virtually divided into four quadrants. A transparent platform (8-cm diameter) was placed about 0.5 cm beneath the water surface. During all test sessions, the platform was located in the southwest quadrant of the pool. Each mouse had to perform three trials with a time lag of 10 minutes in between (intertrial time) on each of 4 consecutive days. A single trial lasted for a maximum of 1 minute. During this time, the mouse had to find the hidden, diaphanous platform. After each trial, mice were allowed to rest on the platform for 10–15 seconds to orientate in the surroundings. At least 1 hour after the last trial on day 4, mice had to fulfill a probe trial (PT). During the PT, the platform was removed from the pool, and the number of crossings over the former target position and the abidance in this quadrant were recorded.

A computerized tracking system was used for the quantification of the escape latency (time in seconds the mouse needs to find the hidden platform and, therefore, to escape from the water) and of the

TABLE 1
Binding constants of PQ912 for glutaminyl cyclases determined by enzyme kinetics (K_i, see Fig. 1 for an example) or by SPR (K_D)

Species	PQ912 K_i Determined Kinetically[a]		PQ912 Kinetic Constants Determined by SPR at pH 7.6		
	pH 6.0	pH 8.0	K_D	k_{on}	k_{off}
	nM	nM	nM	$M^{-1}s^{-1}$	s^{-1}
Human QC	19 ± 3[b]	25 ± 3	17	1.3e6	2.3e−2
Mouse QC	41 ± 3	62 ± 7	nd	nd	nd

nd, not determined; SPR, surface plasmone resonance.
[a]For enzyme kinetic measurements of QC, two different batches of PQ912 free base were analyzed. For each batch and each pH value, three separate weighings were performed and analyzed as described in *Materials and Methods*; K_i determination with SPR for human QC were done once.
[b]Mean ± standard deviation.

target-zone crossings and the abidance in the target quadrant in the PT. All animals had to perform a visual test after the PT to rule out visual impairments that may influence the results of the MWM test.

Tissue Sampling. Blood (plasma), cerebrospinal fluid (CSF), and brain samples were collected from Tg mice. Mice were sedated by standard inhalation anesthesia (Isoba, Essex Tierarznei, Munich, Germany). Cerebrospinal fluid was obtained by blunt dissection and exposure of the foramen magnum. Upon exposure, a Pasteur pipette was inserted to an approximate depth of 0.3–1 mm into the cisterna magna. CSF was collected by suction and capillary action until flow fully ceased. CSF samples were immediately frozen on dry ice and stored at −80°C. After CSF sampling, each mouse was placed in dorsal position, the thorax was opened, and a 26-gauge needle attached to a 1-cc syringe was inserted into the right cardiac ventricular chamber. Blood was collected into EDTA-coated vials and used to obtain plasma. To obtain plasma, blood samples from each mouse were centrifuged (1000 × *g*, 10 minutes, room temperature). Following blood sampling, mice were transcardially perfused with physiologic (0.9%) saline. Thereafter, brains were removed, and the cerebellum was cut off and stored at −80°C. Brains were hemisected and immediately frozen on dry ice. One brain hemisphere was used for determination of Aβ level by ELISA, and cerebellum and CSF were used for measurement of compound exposure using liquid chromatography–tandem mass spectrometry (LC-MS/MS).

Analysis of N3pE-Aβ42. Brain tissue without cerebellum was homogenized in Tris-buffered saline [TBS, 20 mM Tris, 137 mM NaCl (pH 7.6), 2 volumes of buffer per brain weight, Dounce homogenizer] containing protease inhibitor cocktail (Complete Mini; Roche, Basel, Switzerland) and 0.1 mM 4-(2-Aminoethyl)benzensulfonylfluorid (Carl Roth, Karlsruhe, Germany), sonicated, and centrifuged at 75,500 × *g* for 1 hour at 4°C. The supernatant was stored at −80°C, and Aβ peptides were sequentially extracted with 2.5 ml of TBS/1% Triton X-100 (TBS/Triton fraction), 2.5 ml of 2% SDS in distilled water (SDS fraction), and 0.5 ml of 70% formic acid (FA fraction). The formic acid extract was neutralized by addition of 3.5 M Tris solution and diluted to a final volume of 10 ml using ELISA blocking buffer (catalog no. 37571; ThermoFisher Scientific). The sum of Aβ determined in the SDS and FA fractions was considered as the insoluble pool of Aβ. ELISAs detecting Aβ(x-42) and N3pE-Aβ42 (IBL-Hamburg) were performed according to the manufacturer's manual. Samples were diluted to fit within the range of the standard curve using assay buffer solution, which is supplied with the ELISA kits. Values below the limit of quantification were set to zero.

Statistics

Descriptive statistical analysis was performed on all evaluated parameters. Data were averaged and (if not stated otherwise) represented as the mean ± S.E.M. Differences compared with respective control groups were analyzed by *t* test or analysis of variance (ANOVA). In the case of non-normally distributed data, Kruskal-Wallis test was used. Post-hoc comparisons with the respective control group were done by Dunnett's or Dunn's test. For the MWM, outliers detected with Grubb's test were excluded from data analysis. Differences in MWM learning curves were evaluated by a two-way ANOVA followed by Dunnett's post-test.

Pharmacokinetics

Pharmacokinetics Day Profile in CSF and Brain after 1 Week of Treatment. PQ912 exposure was determined in a satellite experiment using 10-month-old $hAPP_{SL}$xhQC mice (n = 5 per time point) treated for 1 week with chow (ad libitum) containing 0.8 g/kg PQ912 (equivalent to approximately 200 mg/kg/day). On the last day, animals were sacrificed at 5 a.m., 9 a.m., 1 p.m., 7 p.m., and 11 p.m. CSF, brain, and cerebellum were analyzed for PQ912 using LC-MS/MS as described later.

PQ912 Concentrations in Brain and CSF after Long-Term Treatment. PQ912 exposure was determined in the cerebellum and CSF of $hAPP_{SL}$xhQC mice treated for 6 months with chow (ad libitum) containing 0.24, 0.8, and 2.4 g/kg PQ912. Animals were sacrificed in the morning after 6 weeks (0.8 g/kg only) or 6 months of treatment, and CSF and cerebellum samples were analyzed for PQ912 using LC-MS/MS.

Determination of Free Brain Concentration. The free concentration of PQ912 in brain was determined using equilibrium dialysis in vitro. PQ912 (1 μM final concentration) was spiked into buffer-diluted mouse brain homogenate and buffer and added to either side of the membrane of the rapid equilibrium device (RED;

TABLE 2
Human APP constructs used in cell culture experiments

Construct	APP Sequence[a] at BACE1 Cleavage Site	Aβ Peptide Released after BACE1 Cleavage	Used in Cell Culture Experiments
hAPPwt	593 …EVKM/DAEFRH DSGYEVHHQKL VFFAEDVGSN KGAIIGLMVG GVV… 635	**Aβ(1-40)** DAEFRHDSGY EVHHQKLVFF AEDVGSNKGA IIGLMVGGVV	
APP-NLE	593 …EV**NL**/EFRHD SGYEVHHQKLV FFAEDVGSNK GAIIGLMVGG VV… 635	**Aβ(3-40)** EFRHDSGY EVHHQKLVFF AEDVGSNKGA IIGLMVGGVV	X
APP-NLQ	593 …EV**NL/Q**FRHD SGYEVHHQKLV FFAEDVGSNK GAIIGLMVGG VV… 635	**Aβ(Q3-40)** QFRHDSGY EVHHQKLVFF AEDVGSNKGA IIGLMVGGVV	X

[a]Numbering refers to human APP695 wt variant, Frame and slash: BACE1 cleavage site; bold: amino acid exchange compared with wild-type (wt) sequence.

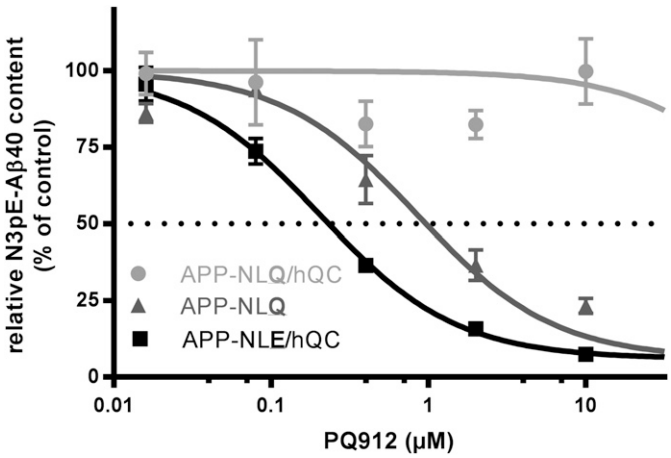

Fig. 2. Inhibition of QC-catalyzed N3pE-Aβ40 formation by PQ912 in cell culture (means ± S.E.M. and four-parameter fits) with the following constraints for all curves: top = 100%, bottom = 6%, hillslope = 1. HEK293 cells were transfected to express APP-NLE or APP-NLQ constructs alone or together with human QC. The cells generate E3-Aβ40 (NLE) or Q3-Aβ40, respectively. Hence, QC catalyzes either cyclization of N-terminal glutamate (E-) or glutamine (Q-) residues. We determined EC_{50} of 200 and 800 nM for PQ912-mediated reduction of N3pE-Aβ40 from APP-NLE/hQC and APP-NLQ, respectively. Inhibition of Q-cyclization in the QC-overexpressing model (APP-NLQ/hQC) was negligible ($EC_{50} \gg 10\ \mu M$). The results support a higher potency of PQ912 to inhibit cyclization of glutamic acid residues.

ThermoFisher Scientific, Darmstadt, Germany). After equilibration at 37°C for 4 hours, the compound concentration on both sides of the membrane was analyzed by LC-MS/MS, and the unbound fraction was calculated following correction for the dilution factor.

Bioanalysis with LC-MS/MS. Brain hemispheres or cerebellum samples were homogenized in 2-volume equivalents of 90% acetonitrile using a Precellys 24 homogenizer (Bertin Instruments, Montigny-le-Bretonneux, France) containing 1.4-mm ceramic beads. After centrifugation, the supernatant was further diluted with 90% acetonitrile containing the stable isotope-labeled internal standard.

CSF and in vitro samples were extracted with 3-volume equivalents of acetonitrile containing the stable isotope-labeled internal standard.

Quantification of PQ912 in CSF, brain homogenate, and buffer extracts was done using a specific and sensitive LC-MS/MS method. After protein precipitation and centrifugation, an aliquot of extracts (2 μl) was injected into a Synergi Polar RP column (50 × 2 mm, 2.5 μm; Phenomenex, Torrance, CA) and separated using a linear gradient of water/acetonitrile from 5 to 95% organic within 4 minutes at 0.3 ml/min (HP1200; Agilent, Santa Clara, CA). PQ912 was quantified in the selected reaction-monitoring mode (mass transition 337.4 > 160.1 Da) using either an API3200 or API4000 (Sciex, Framingham, MA) with heated electrospray ionization in positive ion mode. The lower limit of quantification was defined with 0.25 ng/ml, and all six QC samples (low, medium, high), analyzed within each analytical batch, were valid according to bioanalytical guidelines (U.S. Department of Health and Human Services et al., 2001).

Calculation of Target Occupancy. Mean target occupancy was calculated according to the following formula: target occupancy as a percentage = 100*C/(K_i + C), where C is the free concentration of PQ912. The free (unbound) concentration in brain was determined by equilibrium dialysis. K_i represents the inhibitory constant of PQ912 for human QC. The transgenic mice used in the studies were transgenic for human QC, which is specifically expressed in and mainly responsible for pE-Aβ formation in these mice.

Secondary Pharmacology

To assess an influence of treatment on pE-hormone maturation, we determined the concentration of the hormones testosterone and thyrotropin (TSH) and thyroxine (T4) in plasma. The production of the thyroid and the gonadal hormones is regulated by the hypothalamic-pituitary-thyroid (HPT) and the hypothalamic-pituitary-gonadal (HPG) axes, respectively. Mice (C57/Bl6) were treated orally for 2 weeks, receiving food pellets containing PQ912 at doses of 2.4 and 4.8 g/kg. Afterward, animals were sacrificed and blood plasma was prepared. Specific ELISAs were used according to the manufacturer's instructions for determination of TSH (#SY45021; Cusabio, College Park, MD), T4 (#RE55261), and testosterone (#RE52151; IBL).

Results

In Vitro Binding Studies

Mammalian glutaminyl cyclases are metalloenzymes that contain a typical architecture of a catalytic zinc-binding motif. PQ912 showed competitive inhibition of human QC activity (Fig. 1) with a K_i value of about 25 nM (pH 8.0). Similar K_i values were found for inhibition of recombinant murine QC (Table 1). The binding constant of PQ912 for human QC was also determined using surface plasmon resonance (SPR) technology. PQ912 showed fast association and dissociation kinetics with a K_D value of 17 nM. The k_{off} value of 0.023 $second^{-1}$ corresponds to a half-life of the QC-inhibitor complex of about 30 seconds.

Cellular Assays

The effect of human QC inhibition on formation of N3pE-Aβ40 was determined using a cellular assay, which is based on expression of human APP695 variants (Table 2) together with QC (Cynis et al., 2008). HEK293 cells expressing human APP-NLE and human QC were used to determine the potency of PQ912 (Fig. 2). The APP-NLE construct leads to formation of E3-Aβ40/42 by BACE1 and γ-secretase cleavage of APP. Human QC converts the N-terminal glutamate residue to form N3pE-Aβ40/42. With overexpression of APP-NLE alone (without QC overexpression), there was no pE-Aβ detectable within an acceptable time frame for the cell-culture experiment. Therefore, the APP-NLE/hQC model was used to investigate the effect of QC inhibitors on Glu cyclization. The EC_{50} values for PQ912 to inhibit N3pE-Aβ40/42 formation in the APP-NLE/hQC model were determined to be in the range of 0.14–0.25 μM. Figure 2 shows an experiment in which the APP-NLE/hQC model is directly compared with the APP-NLQ and APP-NLQ/hQC models. In the case of an N-terminal glutamine residue, the inhibitory potency of PQ912 on pE-Aβ formation in the comparable APP-NLQ/hQC model was very low (no noteworthy inhibition up to 10 μM). Also, for inhibition of glutaminyl cyclization in the APP-NLQ model without QC overexpression (only intrinsic cellular QC activity), about 4-fold higher inhibitor concentrations are needed (EC_{50} = 0.8 μM) compared with the APP-NLE/hQC model. These observations point toward a higher potency to inhibit cyclization of glutamate compared with glutamine residues in cell culture. This Glu-Gln potency difference provides an important basis for the target selectivity of the approach.

PQ912 Exposure and Target Occupancy in $hAPP_{SL}$xhQC Mice

The PQ912 exposure in the CSF and brain of $hAPP_{SL}$xhQC mice after oral application of PQ912 (0.8 g/kg chow, ad libitum) is shown in Fig. 3. At this dose, the mean free PQ912 concentration was about 2 times K_i (47 nM for CSF and

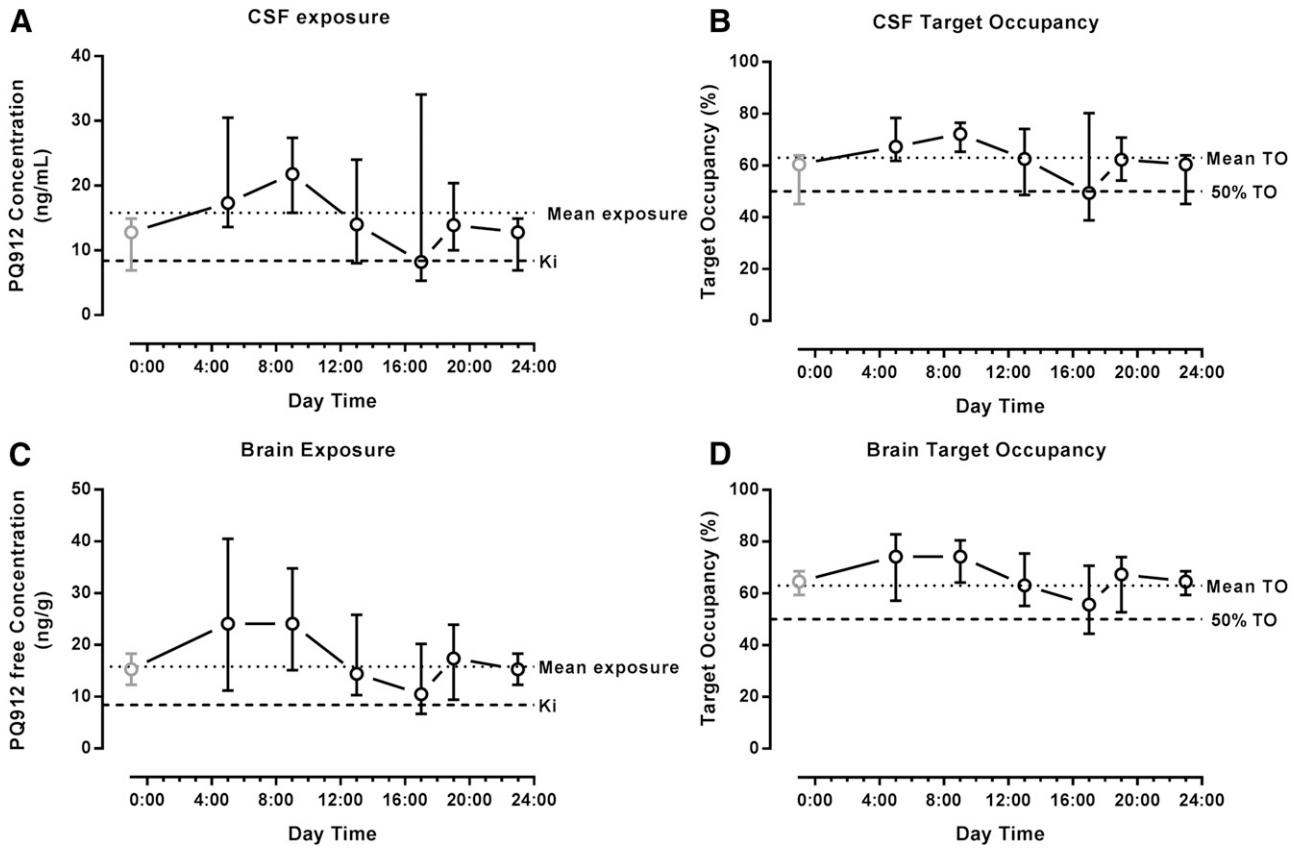

Fig. 3. Time-dependent concentration of free PQ912 in CSF (A) and brain (C) (median ± range, $n = 5$ per time point; data point in gray was extrapolated) and calculated QC target occupancy in CSF (B) and brain (D) after 1 week of PQ912 treatment (0.8 g/kg chow, ad libitum) in 10-month-old $hAPP_{SL}$/hQC mice. The K_i (PQ912) for human QC of 25 nM corresponds to a PQ912 concentration of 8.4 ng/ml. The mean exposure over 24 hours is about 2 × K_i, resulting in a mean target occupancy [TO% = 100*C/(K_i + C)] of about 60%.

56 and 62 nM for brain and cerebellum homogenate, respectively), resulting in a mean target occupancy of more than 60% (65, 69, and 71% for CSF, brain, and cerebellum, respectively).

Previous studies in 5xFAD mice cross-bred with QC knockout mice (Jawhar et al., 2011) implied that more than 50% QC inhibition is required to achieve an effect on pE-Aβ formation and a concomitant behavioral improvement (unpublished observations). Hence, doses of 0.24, 0.8, and 2.4 g were selected for further long-term treatment.

The treatment of $hAPP_{SL}$xhQC mice for 6 months resulted in brain concentrations of about 50, 230, and 700 ng/g brain, respectively (Fig. 4). Considering an unbound fraction of 0.06 ± 0.02 ($n = 3$), the free brain concentrations corresponded well with the PQ912 concentrations in CSF. Thus, these data suggest that an oral dose of 0.8 g/kg is sufficient to achieve more than 60% inhibition of QC in brain over 24 hours.

Pharmacodynamic Effects of PQ912 in Transgenic Mice

Two AD-like mouse models were used to assess the in vivo effect of PQ912: the double-transgenic $hAPP_{SL}$xhQC mice and the 5xFADxhQC mice. The 5xFADxhQC mice were characterized in a previous study (Jawhar et al., 2011). These mice start to develop pE-Aβ–containing deposits at an age of 3–4 months. Also, $hAPP_{SL}$xhQC mice have been briefly described previously (Nussbaum et al., 2012), but a detailed characterization of pE-Aβ deposition and behavioral changes at different ages for these mice was lacking. The development of AD pathology reflected by pE-Aβ increase in the brain and deficits in behavioral tests was evaluated in a longitudinal study as the basis for the definition of prophylactic treatment versus therapeutic treatment paradigms (Fig. 5). PQ912 was then tested for reduction of pE-Aβ formation in $hAPP_{SL}$xhQC

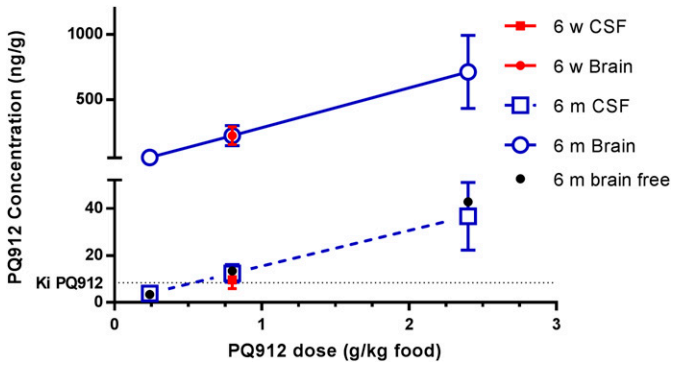

Fig. 4. PQ912 concentrations in brain (circles) and CSF (squares) after 6 months of treatment of $hAPP_{SL}$/hQC mice with 0.24, 0.8, and 2.4 g PQ912/kg chow (ad libitum, n = 11–15 per group, mean ± S.D.). Black-filled circles represent calculated free brain concentrations (f_u = 0.06). Mean compound concentrations in CSF can be translated to approximately 0.45*K_i, 1.47*K_i, and 4.36*K_i, respectively. The red symbols refer to 6-week PQ912 treatment, which results in nearly same brain and CSF levels compared with the 6-month treatment.

or 5xFADxhQC mice in both treatment paradigms. Furthermore, the effect of PQ912 on learning and memory was assessed in the $hAPP_{SL}$xhQC mice.

The deposition of Aβ in $hAPP_{SL}$xhQC transgenic mice starts at an age of about 6 months and increases continuously with age. There was a 3- to 4-fold increase of total Aβ between 9 and 12 months, reaching similar levels in $hAPP_{SL}$ single-transgenic and $hAPP_{SL}$xhQC double-transgenic mice (Fig. 5A). N3pE-Aβ is detectable in some animals above the lower level of quantification for the first time at an age of about 7.5 months and is present in all animals at 9 months of age (Fig. 5B). pE-Aβ progressively accumulates during aging in single-transgenic $hAPP_{SL}$ ($\approx$ 15-fold increase between 9 and 12 months) and especially in the double-transgenic $hAPP_{SL}$xhQC mice ($\approx$ 30-fold increase), resulting in significantly more N3pE-Aβ in the brains of the double-transgenic mice.

First behavioral changes of the double-transgenic mice in the Morris water maze were already detected at 4 months of age (data not shown), thus slightly preceding the presence of pE-Aβ at quantifiable concentrations. Double-transgenic mice perform clearly worse in the Morris water maze between 6 and 9 months of age (Fig. 5, C–F). Therefore, preventive treatment was initiated before the onset of pathophysiological changes, e.g., at an age of 3 months, and therapeutic paradigms began after detection of behavioral or pathologic changes, at 7–8 months of age.

Preventive Long-Term Treatment. In this set of experiments, transgenic mice were treated orally beginning at 3 months of age. PQ912 was applied via food pellets containing 0.24, 0.8, or 2.4 g of compound per kilogram of chow. Behavioral assessment in the Morris water maze test was performed at 8.5 months of age. The animals were sacrificed 2 weeks later, and brain tissue was collected for analysis of compound concentration and Aβ content.

After sacrifice, Aβ was sequentially extracted from brain hemispheres, as described earlier, using TBS, SDS, and formic acid. The concentration of N3pE-Aβ42 within the TBS fraction is depicted in Fig. 6A. The treatment with PQ912 resulted in a significant reduction of N3pE-Aβ42 in the TBS extracts at doses of 0.8 and 2.4 g PQ912 per kilogram of chow. The reduction of N3pE-Aβ42 within the fractions of the insoluble pool (SDS and formic acid summed up) did not reach significance (data not shown).

For the behavioral assessment, wild-type littermates were used as naïve (non-Tg) controls. The effect of PQ912 was compared with vehicle-treated transgenic animals (Tg control). At age 8.5 months, wild-type animals were able to learn to find the target position, whereas vehicle-treated $hAPP_{SL}$xhQC double-transgenic mice showed significant spatial learning impairment measured as longer escape latencies on days 1–4. Treatment with the lowest dose of PQ912 (0.24 g/kg chow) did not show a beneficial effect on learning capabilities. The two higher doses of PQ912 (0.8 and 2.4 g/kg chow) caused a significant amelioration of spatial learning abilities compared with $hAPP_{SL}$xhQC double-transgenic controls, reflected by shorter escape latencies on days 3 and 4 (Fig. 6B, $P < 0.05$ for 0.8-g/kg dose at day 3). In the probe trial, non-Tg controls tended to show better retention abilities reflected by higher abidance in the target quadrant than their vehicle-treated $hAPP_{SL}$xhQC littermates. Treatment with PQ912 showed a dose-dependent trend to enhance the time $hAPP_{SL}$xhQC animals spent in the target zone (ANOVA P value = 0.122) (Fig. 6C).

Therapeutic Short-Term Treatment. In an additional arm of the same study, $hAPP_{SL}$xhQC mice were treated with a PQ912 dose of 0.8 g/kg chow beginning at about 7.5 months of age. The study was performed to assess whether a short treatment period might already result in biochemical changes and a behavioral improvement of the mice. The Morris water maze test was performed after 3 weeks of treatment, thus animal age matched the previous analysis of the preventive long-term treatment. Subsequently, animals (9 months of age) were sacrificed for biochemical analysis. This short-term treatment with the QC inhibitor PQ912 did not affect the N3pE-Aβ42 concentration in brain (Fig. 7A). However, the treatment caused an improvement of spatial learning abilities compared with vehicle-treated $hAPP_{SL}$xhQC double-transgenic controls, shown by significantly shorter escape latencies on day 3 and day 4 (Fig. 7B). With regard to spatial learning, short-term-treated animals showed an abidance in the target quadrant comparable to long-term-treated animals. The effect on spatial memory as assessed in the probe trial did not reach significance (Fig. 7C).

Therapeutic Long-Term Treatment. In an additional set of experiments, we assessed the effect of PQ912 at a dose of 0.8-g/kg food pellets for 4 months, starting at 8 months of age. The treatment resulted in a clear reduction of N3pE-Aβ42 in soluble ($P = 0.052$, t test) and insoluble ($P = 0.022$) Aβ fractions at the 12-month endpoint (Fig. 8, A and B).

We also investigated the effect of PQ912 in 5xFADxhQC mice, which has also been used in a genetic proof-of-concept study (Jawhar et al., 2011). Because these mice start to develop plaques at 2–3 months of age, i.e., earlier than $hAPP_{SL}$xhQC, we treated these animals from 3 to 6 months. The total pE-Aβ load in the brain of vehicle-treated animals was similar to 12-month-old $hAPP_{SL}$xhQC mice (Fig. 8, C and D). Treatment with PQ912 at a dose of 0.8 g of PQ912 per kg chow ($\approx$ 200 mg/kg/day) resulted in a significant reduction of pE-Aβ by about 30% in the TBS (soluble Aβ) as well as the SDS/FA (insoluble Aβ) fraction. Thus, the results obtained with PQ912 in 5xFADxhQC correspond to the results observed in the $hAPP_{SL}$xhQC model.

In Vivo Secondary Pharmacology Related to Substrate Specificity—HPT and HPG Axis. As indicated in the *Introduction*, physiologic substrates of QC carry an N-terminal glutamine (Gln) residue without exception, being cyclized by QC to produce pE at the N terminus. The conversion of N-terminal glutamate residues (Glu), however, seems to be restricted to pathologic situations, such as accumulation of Aβ in AD. To assess an in vivo therapeutic window between pathologic Glu and physiologic Gln cyclization, the effect of PQ912 on testosterone and T4 was measured in male C57/Bl6 mice after 2 weeks of treatment. These hormones function as indicators for the maturation of hypothalamic pE hormones gonadoliberin (GnRH) and thyroliberin (TRH), regulating the HPG or HPT axis, respectively.

Because the pharmacological experiments pointed toward an efficient reduction of pE-Aβ formation and an accompanying behavioral improvement at a dose of 0.8 g PQ912/kg food pellet, 3- and 6-times higher doses of PQ912 were used (2.4 and 4.8 g/kg food pellet). Afterward, animals were sacrificed, and the hormone concentrations in plasma were assessed. With these doses, the downstream hormones of the HPT and

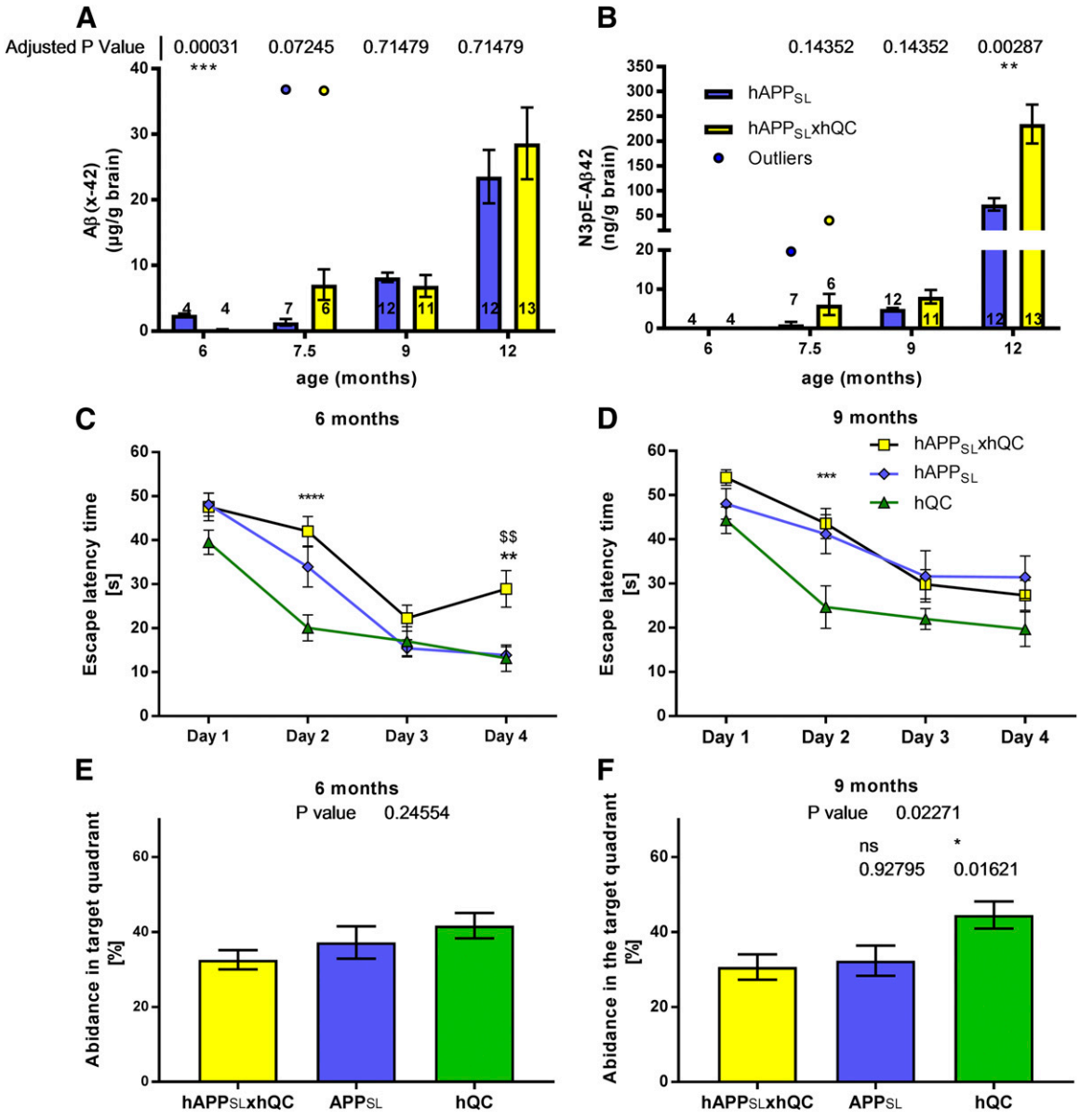

Fig. 5. Characterization of $hAPP_{SL}xhQC$ transgenic mice and littermates. (A and B) Aβ brain levels. Insoluble total Aβ42 (A) and N3pE-Aβ42 (B) concentrations at ages 6, 7.5, 9, and 12 months (n = 4–13 per group, see numbers in columns). Aβ42 was detectable at 6 months in both genotypes (significantly higher in $hAPP_{SL}$) and increased over time. No difference between genotypes was found at 7.5, 9, and 12 months of age. N3pE-Aβ42 becomes detectable for the first time at age 7.5 months in part of the animals (3/8 in $hAPP_{SL}$, 5/7 in $hAPP_{SL}xhQC$). N3pE-Aβ42 increases dramatically between 9 and 12 months (≈ 15-fold in $hAPP_{SL}$, ≈ 29-fold in $hAPP_{SL}xhQC$), resulting in significantly higher N3pE-Aβ42 levels in the double-transgenic animals at 12 months of age. Statistical significance was assessed by multiple t tests (each age, outliers excluded) using the Sidak-Holm method, with α = 0.05 for correction. (C–F) Morris water maze results [escape latency (C and D) and abidance in target quadrant at the probe trial (E and F)] demonstrate that, at an age of 6 (C and E) and 9 months (D and F), $hAPP_{SL}$ single-transgenic and $hAPP_{SL}xhQC$ double-transgenic mice displayed significant impairments in spatial learning and memory compared with nontransgenic (not shown) and hQC single-transgenic animals. For statistical analyses of escape latency curves, two-way ANOVA demonstrates a significant effect of the transgene. Post-hoc comparison of the double-transgenic $hAPP_{SL}xhQC$ group with each single-transgenic group was performed for each time point using Dunnett's multiple comparisons test (α = 0.05) (comparison with *hQC transgenic or APP_{SL} transgenic group; ****adjusted $P < 0.0001$; ***adjusted $P < 0.001$; **adjusted $P < 0.01$). For group comparison of abidance in target quadrant, one-way ANOVA was used (P values at the top of the panels). In post-hoc tests, the double-transgenic group was compared with each single-transgenic group using Dunnett's multiple comparison test. ns, not significant.

HPG axes, testosterone and T4, were not affected by the treatment (Fig. 9).

Discussion

Compelling evidence suggests a crucial role of N-terminally truncated and pE-modified Aβ in Alzheimer's disease (Russo et al., 2002; Gunn et al., 2010; Bayer and Wirths, 2014). These modified peptides have been shown to correlate with progression of AD and tau pathology (Güntert et al., 2006; Mandler et al., 2014; Morawski et al., 2014; Thal et al., 2015). The N-terminal blockage by pE stabilizes against degradation (Saido et al., 1995; Russo et al., 2002) and increases the surface hydrophobicity of oligomeric aggregates, which is most probably linked to toxicity (Schlenzig et al., 2012). It was also shown that pE-Aβ facilitates the formation of

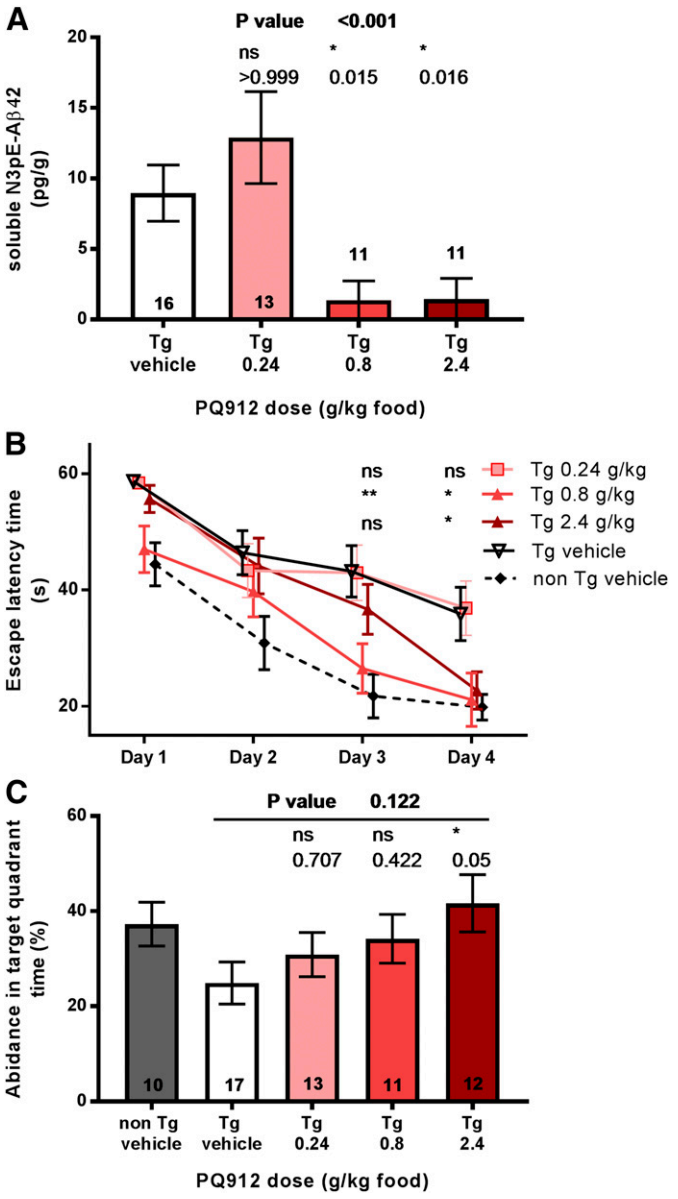

Fig. 6. Analysis of $hAPP_{SL}$xhQC transgenic mice after 6 months of treatment (preventive long-term) with PQ912. (A) Analysis of N3pE-Aβ42 in the TBS fraction (means ± S.E.M., P value at top of graph from Kruskal-Wallis test, adjusted P values from Dunn's multiple comparison with Tg control at top of columns, n per group is given within columns). The treatment resulted in significant reduction ($\alpha = 0.05$) of soluble N3pE-Aβ by 0.8 and 2.4 g PQ912/kg chow. (B and C) Results of Morris water maze assessment of spatial learning and memory. (B) Escape latency on days 1–4 of non-Tg controls (dashed line), $hAPP_{SL}$xhQC controls (black line), and PQ912-treated $hAPP_{SL}$xhQC mice receiving 0.24 (pink line), 0.8 (red line), and 2.4 g/kg chow (dark-red line) for 6 months starting at 3 months of age. Each point represents the mean ± S.E.M. of three trials of all animals in a group per day. A significantly improved performance in the mid- and high-dose groups was observed (ns, not significant; $^*P < 0.05$; $^{**}P < 0.01$) on days 3 and 4 (Dunnett's test for multiple comparison with Tg vehicle-treated group). (C) Abidance in the target quadrant of non-Tg controls (gray), $hAPP_{SL}$xhQC controls (white), and PQ912-treated $hAPP_{SL}$xhQC mice (start of treatment at 3 months of age) receiving 0.24 g/kg (pink), 0.8 g/kg (red), and 2.4 g/kg (dark red) (means ± S.E.M., P value at top is from ANOVA, at top of columns is significance summary with adjusted P values, Dunnett's multiple comparison test with Tg control, n per group is given within columns). A significant effect of high dose was observed ($\alpha = 0.05$).

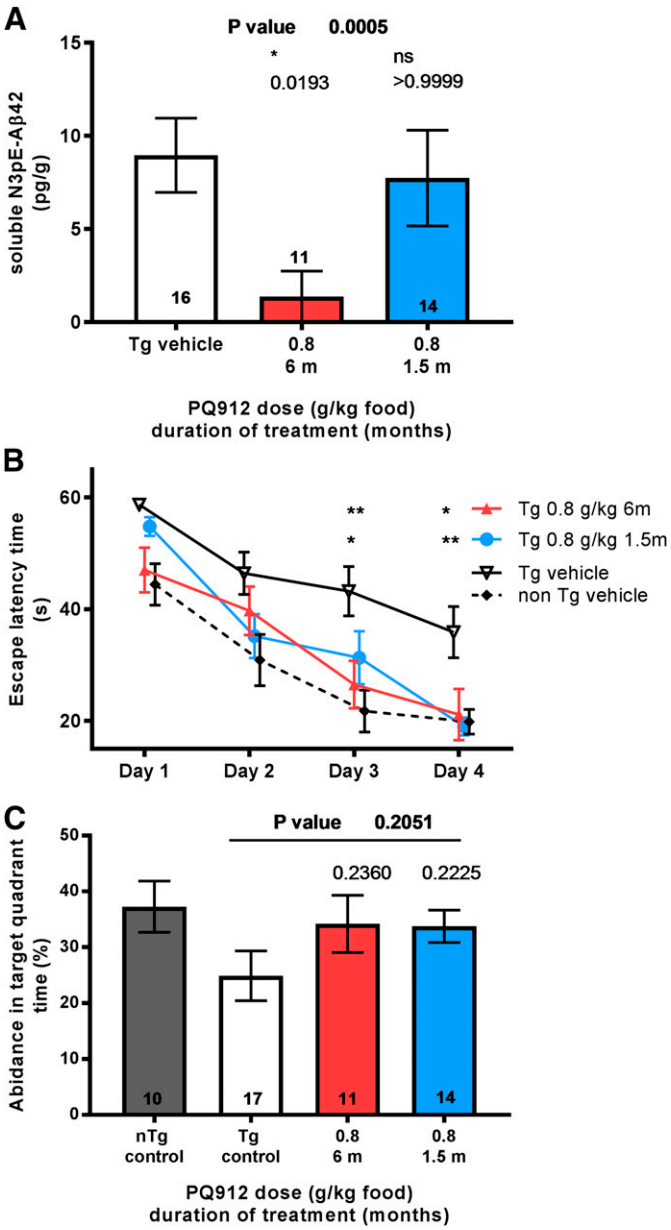

Fig. 7. Analysis of $hAPP_{SL}$xhQC transgenic mice after 6 months (preventive long-term, start at 3 months of age, red) and 1.5 months (therapeutic short-term, start at 7.5 months of age, blue) of treatment with 0.8 g PQ912/kg chow. (A) Analysis of N3pE-Aβ42 in the TBS fraction (means ± S.E.M., P values at top of graph are from Kruskal-Wallis test, at top of columns are significance summary with adjusted P values, Dunn's multiple comparison with Tg control, n per group is given within columns). (B and C) Morris water maze assessment of spatial learning and memory. (B) Escape latency on days 1–4 of non-Tg controls (dashed line), $hAPP_{SL}$xhQC controls (black line), and PQ912-treated $hAPP_{SL}$xhQC mice, treated for 6 (red) or 1.5 (blue) months with 0.8 g/kg. Each point represents the mean ± S.E.M. of three trials of all animals of a group per day. At days 3 and 4, significantly better performance was observed for both treatment regimens ($^*P < 0.05$; $^{**}P < 0.01$; Dunnett's test for multiple comparison with Tg vehicle-treated group). (C) Abidance in the target quadrant of non-Tg controls (gray), $hAPP_{SL}$xhQC controls (white), and $hAPP_{SL}$xhQC mice treated with PQ912 (0.8 g/kg) for 6 (red) or 1.5 (blue) months (means ± S.E.M., P value at top is from ANOVA, at top of columns is significance summary with adjusted P values, Dunnett's multiple comparison test with Tg control, n per group is given within columns). ns, not significant.

hetero-oligomers, inducing toxicity in a tau-dependent manner (Nussbaum et al., 2012). The pE modification is catalyzed by glutaminyl cyclases, enzymes that are present in brain and upregulated in AD (Schilling et al., 2008; De Kimpe et al., 2012). Overexpression of QC and Aβ accumulation in transgenic mice has been shown to induce pE-Aβ formation and

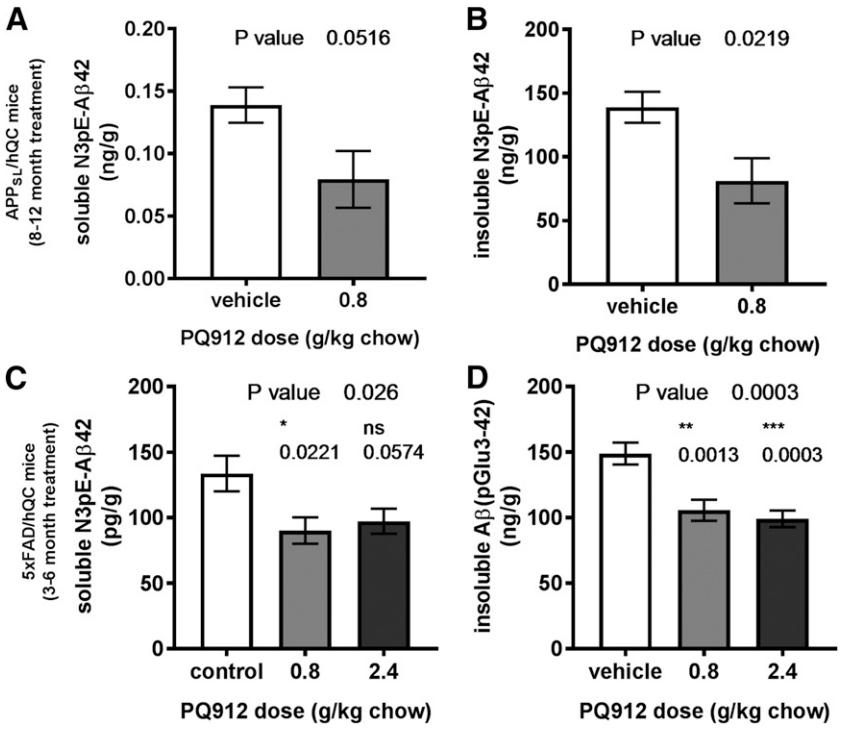

Fig. 8. Analysis of N3pE-Aβ42 after fractionated extraction of Aβ from brains of 12-month-old double-transgenic $hAPP_{SL}$xhQC (A and B) or 6-month-old 5xFADxhQC (C and D) double-transgenic mice (n = 7–8 per group). Oral treatment with PQ912 resulted in robust reduction of N3pE-Aβ42. P values of t test (A and B) or ANOVA (C and D) are given at the top of the graphs. Summary statistics ($^*P < 0.05$; $^{***}P < 0.001$; ns, not significant) and adjusted P values of Dunnett's post-hoc comparison with control group are given at the top of each column (C and D).

behavioral impairment, and a knockout of QC rescued the observed phenotype (Jawhar et al., 2011; Nussbaum et al., 2012). Hence, inhibitors of QC represent potential therapeutics to treat AD. PQ912 is the first inhibitor of QC that entered clinical development. The results of a comprehensive phase 1 study have been recently published (Lues et al., 2015).

The aim of the present study was 2-fold. First, we aimed to determine an effective dose of PQ912, which results in reduction of pE-Aβ formation and concomitant behavioral improvement of transgenic mice. These data provide a key translational finding for the clinical assessment of PQ912 in humans. Second, we addressed a potential functional selectivity for inhibition of pE formation from N-terminal glutamic acid over glutamine. Glutamate3-Aβ represents the precursor of N3pE-Aβ, whereas glutamine is the precursor of N-terminal pE in all physiologic substrates, including TRH and GnRH. Therefore, the results should provide evidence for a reasonable therapeutic window.

To assess the efficacy in vivo, we used the $hAPP_{SL}$xhQC and 5xFADxhQC mouse models. These mice generate pE-Aβ at higher levels than other mouse models, and the appearance of pE-Aβ is linked to behavioral changes in spatial learning and memory, beginning at age 4–6 months (Fig. 5) (Jawhar et al., 2011; Nussbaum et al., 2012). The preventive treatment of $hAPP_{SL}$xhQC mice with an oral PQ912 dose of 0.8 g/kg chow ($\approx$ 200 mg/kg/day) for 6 months starting at 3 months of age resulted in a significant reduction of pE-Aβ formation. The reduction of pE-Aβ was accompanied by an improvement of spatial learning, assessed using a Morris water maze paradigm (Fig. 6). Suppression of pE-Aβ was corroborated in the therapeutic treatment of $hAPP_{SL}$xhQC and 5xFADxhQC mice where 0.8 g PQ912/kg in food pellets caused a significant reduction of pE-Aβ after 4 months of treatment (Fig. 8). The CSF concentration of about 47 nM at the end of the experiment predicted a QC inhibition of about 65%. An effective dose in this range, resulting in >50% target occupancy, is in good agreement with previous results on genetic ablation of QC activity in 5xFAD mice (Jawhar et al., 2011). A 50% reduction of QC activity by heterozygous ablation of QC did not affect pE-Aβ formation and had only weak effects on behavior (unpublished results). In contrast, homozygous depletion of QC resulted in a rescue of the behavioral impairment and a significant reduction of pE-Aβ (Jawhar et al., 2011). This indicates that the average QC inhibition necessary to obtain a robust therapeutic effect should be higher than 50%. Thus, our studies in transgenic mice highlight an effective brain exposure that can be used for translation to human trials. Results of a phase 1 study with PQ912 in healthy volunteers suggested

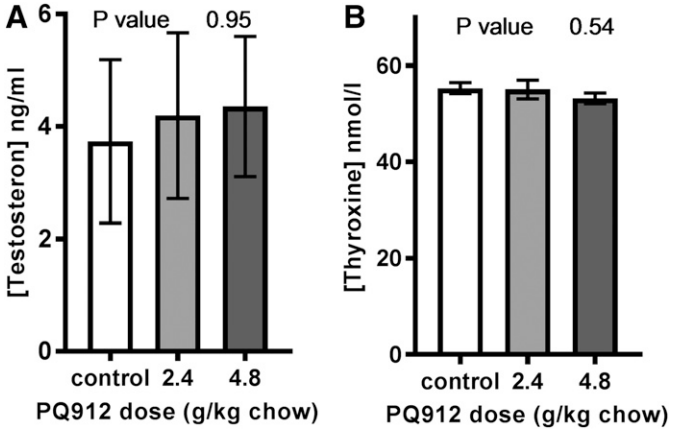

Fig. 9. Analysis of the effect of PQ912 treatment on HPG and HPT axes. Testosterone (A) and thyroxine (T4) (B) concentrations (mean ± S.E.M.) were measured in plasma of 12-week-old male C57/Bl6 mice (n = 17 per group) after treatment with supratherapeutic doses for 2 weeks. An effect on the hormone concentration was not observed, suggesting that a probable inhibition of the maturation of hypothalamic TRH or GnRH by PQ912 is negligible (P values from one-way-ANOVA).

that, with well tolerated doses, an average QC inhibition in CSF of 90% could be achieved (Lues et al., 2015).

QC has physiologic substrates; therefore, it is important to evaluate not only the primary pharmacological effect of the cyclization of the N-terminal glutamic acid residue in N3pE-Aβ, but also the effect of PQ912 on those peptides which carry an N-terminal glutamine residue. Reduction of the pE hormones TRH or GnRH, which are generated from Gln precursors, results in hypothyroidism or hypogonadism, respectively (Mason et al., 1986; Yamada et al., 1997).

Therefore, the preference of PQ912 to inhibit Glu over Gln cyclization was addressed in an HEK cell model overexpressing different APP constructs as precursors of E3- or Q3-Aβ. PQ912 effectively inhibited formation of N3pE-Aβ40 from E3-Aβ40 (APP-NLE/hQC), with an EC_{50} of about 200 nM. However, the cyclization of the N-terminal glutamine residue, which is generated by a mutated APP construct leading to Q3-Aβ instead of E3-Aβ (APP-NLQ), was not inhibited, with at least 50-fold higher PQ912 concentrations and otherwise identical conditions (overexpression of QC).

Different potential reasons could be considered for this apparent selectivity of PQ912 for inhibition of cyclization of glutamic acid residues. First, the difference in the specificity constants of the Glu versus Gln substrates likely play a role. The apparent dissociation constant (K_M) of Glu substrates was shown to be about 3 orders of magnitude higher compared with the respective Gln substrates (Schilling et al., 2004; Seifert et al., 2009). This, in turn, results in enforced competitive replacement of the Glu substrate by the inhibitor, which might account for the apparent specificity of PQ912 to more strongly suppress cyclization of glutamic acid residues. Second, the cyclization of glutamine residues occurs mainly intracellularly, i.e., under conditions of high substrate and enzyme concentrations. Evidence for this was provided by studies on the maturation of peptide hormones (Nillni and Sevarino, 1999; Keire et al., 2003). These peptides are matured within secretory vesicles and are secreted as the modified pE species. Under these high-enzyme/high-substrate conditions, the excess substrate "protects" the enzyme from binding the inhibitor so that much higher inhibitor concentrations are needed for considerable inhibition of the Gln cyclization. Finally, we have previously shown that N-terminal glutamine is prone to spontaneous cyclization with a half-life of several hours. Thus, spontaneous cyclization of N-terminal glutamine residues might also contribute to pE formation in physiologic substrates. In contrast, N-terminal glutamic acid residues cyclize at negligible rates spontaneously (Seifert et al., 2009). All of the aforementioned mechanisms might play a role in vivo, causing a higher potency of QC inhibitors to prevent Glu cyclization.

To translate these findings to physiologic substrates in vivo, the effect of PQ912 on plasma levels of gonadal and thyroid hormones was assessed in mice treated with PQ912. The secretion of T3 and T4 is regulated by the HPT axis, which also consists of the hypothalamic hormone TRH (pyroGlu-His-Pro-amide) and the pituitary hormone TSH. A reduction in mature TRH may occur due to reduction in formation of N-terminal pE in response to QC inhibition. A pronounced reduction of TRH would result in hypothyroidism, as is observed in TRH knockout mice (Yamada et al., 1997). These mice show a 50% reduction of the thyroxine concentration, increased TSH concentration, and hyperglycemia. Homozygous QC knockout mice show a very mild hypothyroidism as suggested by a 20% reduction of thyroxine virtually no effect on TSH, and no hyperglycemia. The effect is likely caused by a reduction of mature pE-TRH (Schilling et al., 2011).

To estimate the therapeutic window based on the differences in inhibition of pE formation in Gln and Glu substrates, we assessed TSH, thyroxine, and testosterone in plasma of mice treated with high doses of PQ912. Importantly, we did not observe an effect on testosterone, nor on the TSH and thyroxine concentration, even after treatment with a dose 6-fold higher than an efficacious pharmacological dose (Fig. 9) necessary for inhibition of pE-Aβ formation. This corresponds with results in the multiple ascending dose phase 1 study, where T3/T4 levels were not affected at a dose, which leads to 90% QC inhibition, on average, in the spinal fluid. Thus, the apparent specificity of PQ912 on cyclization of Glu residues opens a therapeutic window for effectively reducing the pE-Aβ formation without effect on hormonal regulation cascades.

To summarize, our results suggest a robust therapeutic effect of PQ912 in transgenic mouse models of AD. These data further strengthen the hypothesis that the formation of pE-Aβ can be effectively reduced by inhibition of glutaminyl cyclase, and that brain QC is a druggable target. The therapeutic effect of PQ912 is observed at an oral dose of about 200 mg/kg/day, which translates to about 60–70% brain target occupancy. Notably, these observations match very well with a pharmacokinetic/pharmacodynamic relationship in human phase 1 studies, which revealed an EC_{50} of 30 nM in human CSF (Lues et al., 2015). Moreover, the results suggest a comfortable therapeutic window for the compound's primary pharmacological effect on pE-Aβ and behavior in AD animal models versus its effects on hormonal regulation cascades driven by glutamine cyclization.

Acknowledgments

The technical assistance of S. Torkler for cell culture experiments, D. Meitzner and Mirko Müller for bioanalytics, and M. Scharfe and K. Schulz for enzyme kinetics experiments is gratefully acknowledged.

Authorship Contributions

Participated in research design: Hoffmann, Lues, Demuth, Schilling.

Conducted experiments: Meyer, Kurat, Böhme, Kleinschmidt, Farcher.

Performed data analysis: Hoffmann, Schilling, Bühring, Meyer, Hutter-Paier.

Wrote or contributed to the writing of the manuscript: Heiser, Hoffmann, Meyer, Lues, Schilling.

References

Bayer TA and Wirths O (2014) Focusing the amyloid cascade hypothesis on N-truncated Abeta peptides as drug targets against Alzheimer's disease. *Acta Neuropathol* **127**:787–801.

Buchholz M, Hamann A, Aust S, Brandt W, Böhme L, Hoffmann T, Schilling S, Demuth HU, and Heiser U (2009) Inhibitors for human glutaminyl cyclase by structure based design and bioisosteric replacement. *J Med Chem* **52**:7069–7080.

Buchholz M, Heiser U, Schilling S, Niestroj AJ, Zunkel K, and Demuth HU (2006) The first potent inhibitors for human glutaminyl cyclase: synthesis and structure-activity relationship. *J Med Chem* **49**:664–677.

Cynis H, Scheel E, Saido TC, Schilling S, and Demuth HU (2008) Amyloidogenic processing of amyloid precursor protein: evidence of a pivotal role of glutaminyl cyclase in generation of pyroglutamate-modified amyloid-beta. *Biochemistry* **47**: 7405–7413.

De Kimpe L, Bennis A, Zwart R, van Haastert ES, Hoozemans JJ, and Scheper W (2012) Disturbed Ca2+ homeostasis increases glutaminyl cyclase expression; connecting two early pathogenic events in Alzheimer's disease in vitro. *PLoS One* **7**:e44674.

Esparza TJ, Wildburger NC, Jiang H, Gangolli M, Cairns NJ, Bateman RJ, and Brody DL (2016) Soluble Amyloid-beta Aggregates from Human Alzheimer's Disease Brains. *Sci Rep* **6**:38187.

Gillman AL, Jang H, Lee J, Ramachandran S, Kagan BL, Nussinov R, and Teran Arce F (2014) Activity and architecture of pyroglutamate-modified amyloid-β (AβpE3-42) pores. *J Phys Chem B* **118**:7335–7344.

Gunn AP, Masters CL, and Cherny RA (2010) Pyroglutamate-Aβ: role in the natural history of Alzheimer's disease. *Int J Biochem Cell Biol* **42**:1915–1918.
Güntert A, Döbeli H, and Bohrmann B (2006) High sensitivity analysis of amyloid-beta peptide composition in amyloid deposits from human and PS2APP mouse brain. *Neuroscience* **143**:461–475.
Hardy JA and Higgins GA (1992) Alzheimer's disease: the amyloid cascade hypothesis. *Science* **256**:184–185.
Ittner LM and Götz J (2011) Amyloid-β and tau–a toxic pas de deux in Alzheimer's disease. *Nat Rev Neurosci* **12**:65–72.
Jawhar S, Wirths O, Schilling S, Graubner S, Demuth HU, and Bayer TA (2011) Overexpression of glutaminyl cyclase, the enzyme responsible for pyroglutamate Abeta formation, induces behavioral deficits, and glutaminyl cyclase knockout rescues the behavioral phenotype in 5XFAD mice. *J Biol Chem* **286**: 4454–4460.
Keire DA, Vincent Wu S, Diehl DL, Chew P, Ho FJ, Davis MT, Lee TD, Shively JE, Walsh JH, and Reeve, JrJR (2003) Rat progastrin processing yields peptides with altered potency at the CCK-B receptor. *Regul Pept* **113**:115–124.
Kuo YM, Emmerling MR, Woods AS, Cotter RJ, and Roher AE (1997) Isolation, chemical characterization, and quantitation of A beta 3-pyroglutamyl peptide from neuritic plaques and vascular amyloid deposits. *Biochem Biophys Res Commun* **237**:188–191.
Lambert MP, Barlow AK, Chromy BA, Edwards C, Freed R, Liosatos M, Morgan TE, Rozovsky I, Trommer B, Viola KL, et al. (1998) Diffusible, nonfibrillar ligands derived from Abeta1-42 are potent central nervous system neurotoxins. *Proc Natl Acad Sci USA* **95**:6448–6453.
Lemere CA, Blusztajn JK, Yamaguchi H, Wisniewski T, Saido TC, and Selkoe DJ (1996) Sequence of deposition of heterogeneous amyloid beta-peptides and APO E in Down syndrome: implications for initial events in amyloid plaque formation. *Neurobiol Dis* **3**:16–32.
Lues I, Weber F, Meyer A, Bühring U, Hoffmann T, Kühn-Wache K, Manhart S, Heiser U, Pokorny R, Chiesa J, et al. (2015) A phase 1 study to evaluate the safety and pharmacokinetics of PQ912, a glutaminyl cyclase inhibitor, in healthy subjects. *Alzheimer's Dement (N Y)* **1**:182–195.
Mandler M, Walker L, Santic R, Hanson P, Upadhaya AR, Colloby SJ, Morris CM, Thal DR, Thomas AJ, Schneeberger A, et al. (2014) Pyroglutamylated amyloid-β is associated with hyperphosphorylated tau and severity of Alzheimer's disease. *Acta Neuropathol* **128**:67–79.
Mason AJ, Hayflick JS, Zoeller RT, Young, 3rdWS, Phillips HS, Nikolics K, and Seeburg PH (1986) A deletion truncating the gonadotropin-releasing hormone gene is responsible for hypogonadism in the hpg mouse. *Science* **234**: 1366–1371.
Matos JO, Goldblatt G, Jeon J, Chen B, and Tatulian SA (2014) Pyroglutamylated amyloid-β peptide reverses cross β-sheets by a prion-like mechanism. *J Phys Chem B* **118**:5637–5643.
Miravalle L, Calero M, Takao M, Roher AE, Ghetti B, and Vidal R (2005) Amino-terminally truncated Abeta peptide species are the main component of cotton wool plaques. *Biochemistry* **44**:10810–10821.
Morawski M, Schilling S, Kreuzberger M, Waniek A, Jäger C, Koch B, Cynis H, Kehlen A, Arendt T, Hartlage-Rübsamen M, et al. (2014) Glutaminyl cyclase in human cortex: correlation with (pGlu)-amyloid-β load and cognitive decline in Alzheimer's disease. *J Alzheimers Dis* **39**:385–400.
Mudher A and Lovestone S (2002) Alzheimer's disease-do tauists and baptists finally shake hands? *Trends Neurosci* **25**:22–26.
Näslund J, Schierhorn A, Hellman U, Lannfelt L, Roses AD, Tjernberg LO, Silberring J, Gandy SE, Winblad B, Greengard P, et al. (1994) Relative abundance of Alzheimer A beta amyloid peptide variants in Alzheimer disease and normal aging. *Proc Natl Acad Sci USA* **91**:8378–8382.
Nillni EA and Sevarino KA (1999) The biology of pro-thyrotropin-releasing hormone-derived peptides. *Endocr Rev* **20**:599–648.
Nussbaum JM, Schilling S, Cynis H, Silva A, Swanson E, Wangsanut T, Tayler K, Wiltgen B, Hatami A, Rönicke R, et al. (2012) Prion-like behaviour and tau-dependent cytotoxicity of pyroglutamylated amyloid-β. *Nature* **485**:651–655.
Piccini A, Russo C, Gliozzi A, Relini A, Vitali A, Borghi R, Giliberto L, Armirotti A, D'Arrigo C, Bachi A, et al. (2005) beta-amyloid is different in normal aging and in Alzheimer disease. *J Biol Chem* **280**:34186–34192.
Portelius E, Bogdanovic N, Gustavsson MK, Volkmann I, Brinkmalm G, Zetterberg H, Winblad B, and Blennow K (2010) Mass spectrometric characterization of brain amyloid beta isoform signatures in familial and sporadic Alzheimer's disease. *Acta Neuropathol* **120**:185–193.
Ramsbeck D, Buchholz M, Koch B, Böhme L, Hoffmann T, Demuth HU, and Heiser U (2013) Structure-activity relationships of benzimidazole-based glutaminyl cyclase inhibitors featuring a heteroaryl scaffold. *J Med Chem* **56**: 6613–6625.
Rijal Upadhaya A, Kosterin I, Kumar S, von Arnim CA, Yamaguchi H, Fändrich M, Walter J, and Thal DR (2014) Biochemical stages of amyloid-β peptide aggregation and accumulation in the human brain and their association with symptomatic and pathologically preclinical Alzheimer's disease. *Brain* **137**:887–903.
Russo C, Violani E, Salis S, Venezia V, Dolcini V, Damonte G, Benatti U, D'Arrigo C, Patrone E, Carlo P, et al. (2002) Pyroglutamate-modified amyloid beta-peptides–AbetaN3(pE)–strongly affect cultured neuron and astrocyte survival. *J Neurochem* **82**:1480–1489.
Saido TC, Iwatsubo T, Mann DM, Shimada H, Ihara Y, and Kawashima S (1995) Dominant and differential deposition of distinct beta-amyloid peptide species, A beta N3(pE), in senile plaques. *Neuron* **14**:457–466.
Saido TC, Yamao-Harigaya W, Iwatsubo T, and Kawashima S (1996) Amino- and carboxyl-terminal heterogeneity of beta-amyloid peptides deposited in human brain. *Neurosci Lett* **215**:173–176.
Schilling S, Cynis H, von Bohlen A, Hoffmann T, Wermann M, Heiser U, Buchholz M, Zunkel K, and Demuth HU (2005) Isolation, catalytic properties, and competitive inhibitors of the zinc-dependent murine glutaminyl cyclase. *Biochemistry* **44**:13415–13424.
Schilling S, Hoffmann T, Manhart S, Hoffmann M, and Demuth HU (2004) Glutaminyl cyclases unfold glutamyl cyclase activity under mild acid conditions. *FEBS Lett* **563**:191–196.
Schilling S, Hoffmann T, Rosche F, Manhart S, Wasternack C, and Demuth HU (2002a) Heterologous expression and characterization of human glutaminyl cyclase: evidence for a disulfide bond with importance for catalytic activity. *Biochemistry* **41**:10849–10857.
Schilling S, Hoffmann T, Wermann M, Heiser U, Wasternack C, and Demuth HU (2002b) Continuous spectrometric assays for glutaminyl cyclase activity. *Anal Biochem* **303**:49–56.
Schilling S, Kohlmann S, Bäuscher C, Sedlmeier R, Koch B, Eichentopf R, Becker A, Cynis H, Hoffmann T, Berg S, et al. (2011) Glutaminyl cyclase knock-out mice exhibit slight hypothyroidism but no hypogonadism: implications for enzyme function and drug development. *J Biol Chem* **286**:14199–14208.
Schilling S, Zeitschel U, Hoffmann T, Heiser U, Francke M, Kehlen A, Holzer M, Hutter-Paier B, Prokesch M, Windisch M, et al. (2008) Glutaminyl cyclase inhibition attenuates pyroglutamate Abeta and Alzheimer's disease-like pathology. *Nat Med* **14**:1106–1111.
Schlenzig D, Manhart S, Cinar Y, Kleinschmidt M, Hause G, Willbold D, Funke SA, Schilling S, and Demuth HU (2009) Pyroglutamate formation influences solubility and amyloidogenicity of amyloid peptides. *Biochemistry* **48**:7072–7078.
Schlenzig D, Rönicke R, Cynis H, Ludwig HH, Scheel E, Reymann K, Saido T, Hause G, Schilling S, and Demuth HU (2012) N-Terminal pyroglutamate formation of Aβ38 and Aβ40 enforces oligomer formation and potency to disrupt hippocampal long-term potentiation. *J Neurochem* **121**:774–784.
Seifert F, Schulz K, Koch B, Manhart S, Demuth HU, and Schilling S (2009) Glutaminyl cyclases display significant catalytic proficiency for glutamyl substrates. *Biochemistry* **48**:11831–11833.
Selkoe DJ (2008) Soluble oligomers of the amyloid beta-protein impair synaptic plasticity and behavior. *Behav Brain Res* **192**:106–113.
Shankar GM, Li S, Mehta TH, Garcia-Munoz A, Shepardson NE, Smith I, Brett FM, Farrell MA, Rowan MJ, Lemere CA, et al. (2008) Amyloid-beta protein dimers isolated directly from Alzheimer's brains impair synaptic plasticity and memory. *Nat Med* **14**:837–842.
Shirotani K, Tsubuki S, Lee HJ, Maruyama K, and Saido TC (2002) Generation of amyloid beta peptide with pyroglutamate at position 3 in primary cortical neurons. *Neurosci Lett* **327**:25–28.
Thal DR, Walter J, Saido TC, and Fändrich M (2015) Neuropathology and biochemistry of Aβ and its aggregates in Alzheimer's disease. *Acta Neuropathol* **129**:167–182.
U.S. Department of Health and Human Services, Food and Drug Administration, Center for Drug Evaluation and Research, Center for Veterinary Medicine (2001) Guidance for industry: bioanalytical method validation, Food and Drug Administration, Silver Spring, MD.
Wu G, Miller RA, Connolly B, Marcus J, Renger J, and Savage MJ (2014) Pyroglutamate-modified amyloid-β protein demonstrates similar properties in an Alzheimer's disease familial mutant knock-in mouse and Alzheimer's disease brain. *Neurodegener Dis* **14**:53–66.
Yamada M, Saga Y, Shibusawa N, Hirato J, Murakami M, Iwasaki T, Hashimoto K, Satoh T, Wakabayashi K, Taketo MM, et al. (1997) Tertiary hypothyroidism and hyperglycemia in mice with targeted disruption of the thyrotropin-releasing hormone gene. *Proc Natl Acad Sci USA* **94**:10862–10867.

Address correspondence to: Dr. Inge Lues, Probiodrug AG, Weinbergweg 22, 06120 Halle, Germany. E-mail: Inge.Lues@probiodrug.de